Strongly Coupled Plasmas via Rydberg Blockade of Cold Atoms

G. Bannasch,[1] T. C. Killian,[2] and T. Pohl[1]

[1]*Max Planck Institute for the Physics of Complex Systems, D-01187 Dresden, Germany*
[2]*Rice University, Department of Physics and Astronomy and Rice Quantum Institute, Houston, Texas 77251, USA*
(Received 29 January 2013; published 18 June 2013)

We propose and analyze a new scheme to produce ultracold neutral plasmas deep in the strongly coupled regime. The method exploits the interaction blockade between cold atoms excited to high-lying Rydberg states and therefore does not require substantial extensions of current ultracold plasma experiments. Extensive simulations reveal a universal behavior of the resulting Coulomb coupling parameter, providing a direct connection between the physics of strongly correlated Rydberg gases and ultracold plasmas. The approach is shown to reduce currently accessible temperatures by more than an order of magnitude, which opens up a new regime for ultracold plasma research and cold ion-beam applications with readily available experimental techniques.

Strongly coupled Coulomb systems occupy an exotic regime of plasma physics [1–3] where correlated dynamics due to strong interactions dominates random thermal motion of the charges. While plasmas generally constitute the most abundant state of matter [4], strongly coupled systems are rather scarce and typically require extremely high densities that occur in such exotic settings as the interior of stars and giant gas planets [5] or inertial-confinement fusion experiments [6]. On the other hand, ultracold neutral plasmas (UNPs), produced by direct photoionization of laser-cooled atoms [7–9], represent a promising alternative for creating and studying strongly coupled plasmas, which provides unique opportunities to probe dynamical phenomena [8]. Their low temperatures yield strong coupling conditions at such small densities that typical evolution time scales are slowed down tremendously. This has enabled recent experiments to investigate collective excitations [10,11], relaxation processes [12,13], as well as dynamical instabilities [14] at ultralow plasma temperatures. Such conditions also hold great promise for applications in nanotechnology, where UNPs are utilized to create high-brightness ion beams [15–20] for fabricating and characterizing nanoscale objects.

Yet, these intriguing possibilities are currently limited by intrinsic ion heating [21–28] that takes place right after plasma creation. UNPs are produced from ultracold atoms whose initial temperatures suggest extremely strong correlations, which originally raised high hopes for creating neutral plasmas with unprecedented coupling strengths [7]. However, this scheme generates the plasma far from equilibrium in an entirely disordered state, and the subsequent correlation buildup is accompanied by substantial heating that pushes the plasma ions just to the edge of the strong-coupling regime. Theoretical work has suggested ways to suppress this disorder-induced heating (DIH) by introducing initial ion correlations, e.g., by preordering atoms in an optical lattice [29] and by exploiting atomic

correlations in a degenerate Fermi gas [21] or correlations due to Penning ionization of excited atoms [30]. These ideas set challenging experimental demands such as large optical lattices with perfect unit filling of $\sim 10^6$ atoms [29] or very high particle numbers and densities $\sim 10^{13}$ cm^{-3} [21,30], which, thus far, have precluded their experimental implementation.

Here we describe a new UNP-production scheme that strongly suppresses DIH with currently available and well established experimental techniques. The approach is based on the strong correlations between Rydberg atoms that emerge when a cold gas of atoms is laser excited to a high-lying electronic state. The frequency of the excitation laser is shown to permit continuous variation of the plasma coupling strength. This will permit independent control of plasma temperatures and densities, enabling unprecedented studies of the phase diagram [31] of UNPs. Our calculations reveal a universal relation between the plasma's coupling strength and the Rydberg excitation dynamics, suggesting that UNPs could provide a powerful probe of the correlation properties of ultracold Rydberg gases. We demonstrate a maximum suppression of DIH by more than an order of magnitude, which opens up a new regime for UNP research and significantly boosts the brightness and resolution of UNP-based ion beam technology [15].

Figure 1 illustrates the basic idea in comparison to the conventional approach for UNP creation. In the latter case, direct photoionization of cold atoms [Fig. 1(a)] produces a disordered configuration of ions, whose subsequent rearrangement establishes interparticle correlations, and thereby decreases the potential energy of the plasma. Since the total energy is conserved, this leads to a rapid rise of the temperature to $T_i \sim 1$ K, as shown in Fig. 1(f). The corresponding degree of equilibrium correlations can be characterized by the so-called Coulomb coupling parameter $\Gamma = e^2/ak_BT$, where e is the electron charge, k_B is the Boltzmann constant, and $a = ((4/3)\pi\rho)^{-(1/3)}$ is the
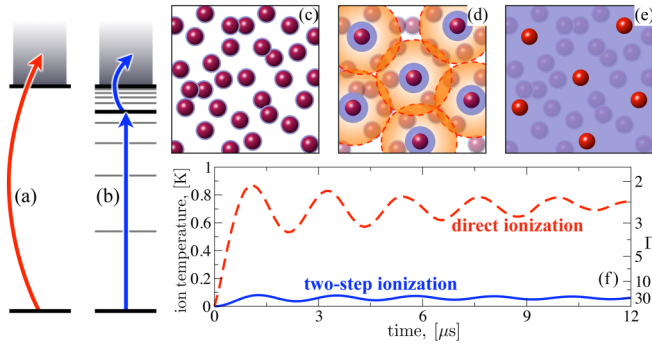
FIG. 1 (color online). Schematics of the (a) conventional direct-ionization scheme for UNP production and (b) the two-step production proposed in this Letter. Starting from a random gas of ground state atoms (c), the latter creates a correlated arrangement of Rydberg atoms (d), whose subsequent ionization results in a correlated plasma (e). As shown in panel (f), these initial correlations substantially suppress DIH after plasma creation (solid line) compared to the conventional production scheme (dashed line). The depicted temperature evolution has been calculated for an initial plasma density of $\rho = 2 \times 10^8 \, \text{cm}^{-3}$ and resonant excitation to $\text{Sr}(100^1 S_0)$ Rydberg states (see text for laser parameters).

Wigner-Seitz radius for a plasma of density ρ. A plasma is termed strongly coupled, when the average potential energy $\sim e^2/a$ of the charges exceeds their thermal energy $\sim k_B T$, i.e., when $\Gamma > 1$. Starting from a random distribution of almost stationary ions, the subsequent equilibration and DIH establishes a Coulomb coupling parameter of $\Gamma \approx 2$ irrespective of the initial ion density and atom temperature [24,25,28] [cf. Fig. 1(f)]. This strong heating can be reduced with a two-step ionization scheme [see Fig. 1(b)], where the ground state atoms are first excited to high-lying Rydberg states and subsequently ionized. In the first excitation step we take advantage of the so called Rydberg blockade [32], which prevents simultaneous excitation of nearby atoms due to the enormous van der Waals interaction between Rydberg atoms [33]. As illustrated in Fig. 1(d), this gives rise to strong Rydberg-Rydberg atom correlations. Their subsequent ionization [34] may, thus, produce a precorrelated plasma [Fig. 1(e)] that evolves into an equilibrium state with a much higher Coulomb coupling parameter [Fig. 1(f)]. We find that, upon rapid ionization, the final plasma correlation function indeed resembles that of the prepared Rydberg gas [see Fig. 2], and shows pronounced oscillations characteristic of a strongly coupled Coulomb liquid.

The Rydberg blockade effect has been the basis of recent experimental breakthroughs for applications in quantum information [35–37] and nonlinear quantum optics [38–43], and has opened the door for studies of quantum many-body phenomena [44–49]. While most of these experiments utilize alkaline atoms, we focus here on cold strontium atoms whose secondary valence electron provides a viable way to probe the temperature of the created plasma
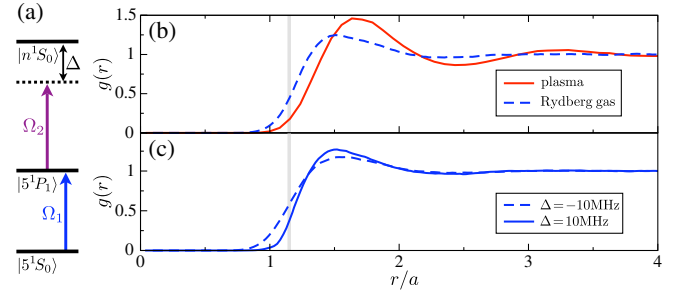

FIG. 2 (color online). (a) Schematic level diagram for two-photon Rydberg excitation. (b) Correlation function $g(r)$ for the Rydberg ensemble and the resulting plasma after relaxation for the same parameters as in Fig. 1(f). The vertical line marks the blockade radius according to Eq. (2). (c) Correlation function of the Rydberg ensemble for two different laser detunings Δ.

ions via optical absorption and fluorescence measurements [23,26,50]. Following recent experiments on Sr-Rydberg gases [51–53], we consider resonant two-photon excitation from the $\text{Sr}(5^1 S_0)$ ground state to a $\text{Sr}(n^1 S_0)$ Rydberg state via the intermediate $\text{Sr}(5^1 P_1)$ state by two excitation lasers with Rabi frequencies Ω_1 and Ω_2 and a two-photon detuning Δ [see Fig. 2(a)]. The single-atom steady state excitation fraction $P_{\text{Ryd}} = \Omega_1^2/(\Omega_1^2 + \Omega_2^2)$ needs to be high in order to maximize interaction effects. We, therefore, choose $\Omega_1 = 25 \, \text{MHz}$ and $\Omega_2 = 0.5$ MHz, which gives $P_{\text{Ryd}} \approx 1$ and can be realized in current experiments [51,52]. Due to the large decay rate $\gamma = 30.2$ MHz of the intermediate state, the resulting many-body excitation dynamics can be described in terms of transition rates [54,55]. The corresponding set of rate equations can be solved efficiently via classical Monte Carlo simulations that account for the Rydberg-Rydberg atom interaction via an effective detuning [54,55]

$$\tilde{\Delta}_i = \Delta - \sum_{j \neq i} \frac{C_6}{|\mathbf{r}_i - \mathbf{r}_j|^6} \qquad (1)$$

of the ith atom at position $\mathbf{r}_i$, where the sum runs over all atoms that are in the Rydberg state. This approach has been applied to study cold Rydberg gases [54–56] and lattices [54,56–58] and was shown to yield good agreement with quantum calculations [55,57]. The van der Waals coefficient $C_6 \sim n^{11}$ strongly increases with the atom's principal quantum number n. Hence, for highly excited states with $n = 100$ the C_6 coefficient of $\text{Sr}(n^1 S_0)$ Rydberg states [59,60] takes on enormous values of $C_6 \approx 20 \, \text{THz} \cdot \mu\text{m}^6$. As a result, a single Rydberg atom can inhibit the excitation of up to a few 10^3 atoms for typical Sr-MOT densities between $\rho_0 = 10^{10} \, \text{cm}^{-3}$ and $\rho_0 = 10^{12} \, \text{cm}^{-3}$ [61–63]. This implies a large number of ground state atoms required to obtain sufficiently many Rydberg excitations. Such sizable ensembles can be described by the Monte Carlo procedure, which allows us to treat up to several 10^7 atoms. Typical simulation results are illustrated in Fig. 2, where we show the Rydberg-Rydberg atom correlation function after

laser excitation. At short distances, simultaneous excitation is completely suppressed by the interaction blockade [32]. The corresponding blockade radius

$$r_b = \left(\frac{C_6}{\hbar \Delta \nu} \right)^{1/6} \qquad (2)$$

can be estimated by equating the respective interaction energy with the linewidth $\Delta \nu$ [64] of the Rydberg excitation. This simple relation yields a good description of the numerical results in Fig. 2 and generally gives $r_b \approx 1.2a$, which is close to the typical correlation length of a strongly coupled plasma.

The conversion of these atomic correlations into ionic ones, requires rapid and efficient ionization of the Rydberg states while leaving the ground state atoms undisturbed. To this end, we consider ionization by a short electric field pulse, which we describe by classical trajectory Monte Carlo (CTMC) simulations [65]. We assume a simple pulse shape $F = F_0 \cos(\omega t + \phi) \exp(-t^2/\tau^2)$, where F_0 denotes the field amplitude and ω, ϕ and τ parametrize the form of the pulse [cf. Fig. 3(a)]. Typical pulse durations τ are on the order of 10^2 ps such that ionic motion and electronic collision processes play no role during field ionization. In addition, the ionization processes has to fulfill two major requirements: (i) ionization needs to be efficient to maximize the transfer of the Rydberg atom ordering into ionic correlations and (ii) the excess energy E_e of the ionized electrons should be sufficiently low so that they remain trapped in the collective ionic space charge potential to form a neutral plasma state [7]. As shown in Fig. 3(b) both conditions are met for a range of $0.1 \lesssim \phi/2\pi \lesssim 0.4$, where we find nearly 100% ionization of $Sr(70^1S_0)$ Rydberg states and an electron kinetic energy below $\sim 10^3$ K. This energy is low enough to enable plasma formation [7] but sufficiently high to prevent rapid
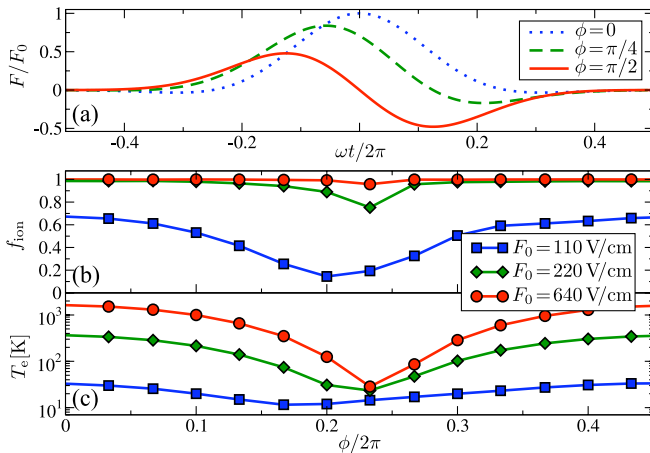
recombination after plasma creation [66–70]. These general conditions can be fulfilled with other pulse shapes different from the one of Fig. 3(a), such as, e.g., half-cycle pulses as demonstrated experimentally in [71].

Finally, we performed molecular dynamics simulations [72] to investigate the subsequent relaxation of the plasma, which is described as a one-component system [73] of initially stationary ions, whose initial positions correspond to those of the Rydberg atoms obtained from the Monte Carlo simulations of the excitation step. Such simulations yield the temperature dynamics shown in Fig. 1(f), which demonstrates a more than tenfold enhancement of the Coulomb coupling parameter. This places the produced plasma deep into the strongly coupled regime with strong liquidlike correlations [see Fig. 2(a)].

The described production scheme involves several parameters that can be widely tuned experimentally. To elucidate their effects we have determined the achievable coupling strengths Γ for various combinations of the ground state atom density ρ_0, the addressed Rydberg level n, and the detuning Δ of the Rydberg excitation laser. For fixed $t_{\rm exc} = 0.5$ μs and resonant excitation, the Coulomb coupling parameter Γ increases with both the atomic density ρ_0 and the principal quantum number n of Rydberg state [Fig. 4(a)]. This behavior can be qualitatively understood from the increasing degree of correlations in cold Rydberg gases with ρ_0 and the strength of the van der Waals interactions. We can quantify this relation by defining the number of blockaded atoms

$$N_b = \frac{4}{3} \pi r_b^3 \rho_0, \qquad (3)$$

which corresponds to the total number of atoms within one blockade sphere of radius r_b. Indeed all data points
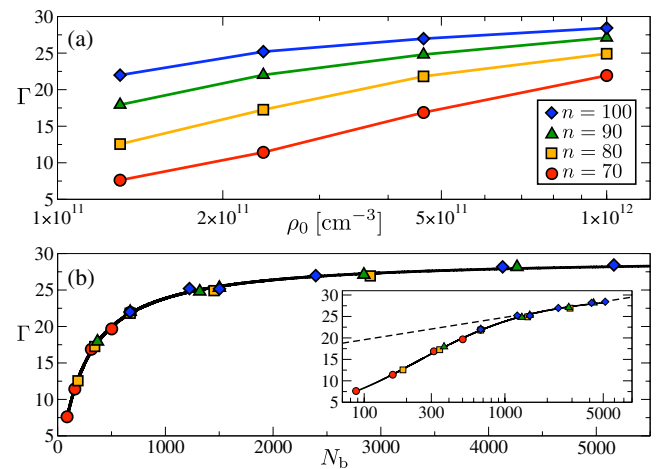

FIG. 3 (color online). (a) Considered shape of the field pulse for Rydberg atom ionization with $\tau = 2\pi/5\omega$. (b) Ionization fraction, $f_{\rm ion}$, and (c) electron temperature, T_e, for $2\pi/\omega =$ 100 ps, $n = 70$ and different values of F_0.

FIG. 4 (color online). (a) Final Coulomb coupling parameter Γ as a function of the ground state atom density ρ_0 for $t_{\rm exc} =$ 0.5 μs and different Rydberg levels n. (b) Same data, but as a function of the number N_b [Eq. (3)] of blocked atoms. The inset demonstrates the logarithmic scaling (dashed line) of Γ.
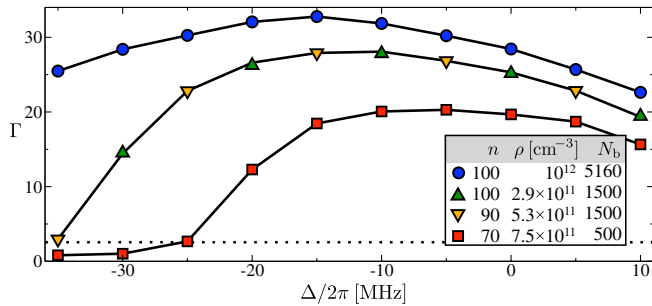
FIG. 5 (color online). Coulomb coupling parameter Γ as a function of laser detuning Δ for $t_{exc} = 0.5$ μs and different combinations of n and ρ_0. The horizontal dotted line shows the Coulomb coupling parameter for direct ionization. Up and down triangles show results for different combinations of ρ and n but identical N_b, demonstrating that the universal scaling [cf. Fig. 4(b)] also holds off resonance.

collapse on a single universal curve as a function of N_b [see Fig. 4(b)]. In the strong blockade limit Γ shows a weak logarithmic growth with N_b such that further increase of the ground state atom density does not yield a substantial enhancement.

However, the detuning of the Rydberg excitation laser provides another control parameter to tune the Coulomb coupling strength. This is demonstrated in Fig. 5 where we show Γ as a function of Δ for different ground state densities and Rydberg states. As seen from Fig. 5, the universal scaling also holds off resonance, such that the final result is determined by Δ and N_b only. For the attractive interactions between $Sr(n^1S_0)$ atoms [59,60] a finite laser detuning gives rise to interaction-induced resonances at the red side of the excitation line ($\Delta < 0$), where Rydberg excitation is enhanced for configurations where $\tilde{\Delta}_i \approx 0$. This additional distance selectivity can produce a more pronounced peak structure of the correlation function [74] and tends to steepen its drop around r_b [see Fig. 2(b)]. As a result the Coulomb coupling parameter can be increased by tuning to the red side of the atomic resonance. For large N_b it assumes a maximum around $\Delta = -\gamma/2$ and drops at either side of the atomic line. Well off resonance, DIH is even enhanced, such that Γ can be tuned from the weak-to-moderate coupling region deep into the strong coupling regime with maximal Coulomb coupling parameters around $\Gamma \sim 35$.

The proposed scheme, therefore, represents a viable way to not only tremendously boost currently achievable coupling strength but also to independently tune the plasma parameters of UNPs, which would otherwise be constrained to $\Gamma = 2 \propto \rho^{1/3}T$. The demonstrated tenfold cooling directly translates into an enhanced brightness of UNP-based ion beams, which enhances the spatial beam resolution [15] for nanotechnology applications.

We have focussed on electric-field ionization of the Rydberg gas, but other approaches for plasma-conversion should also be possible, such as long-wavelength photoionization or electron impact ionization. As pointed out recently [34], the latter occurs naturally in dense Rydberg gases, driving a spontaneous avalanchelike evolution to a plasma [75–79] that could inherit residual Rydberg atom correlations. Spontaneous plasma formation, however, takes place on long microsecond time scales [34,75] and involves significant atomic motion [80] and loss of highly excited atoms to low-lying states [76,77]—all of which deteriorate the cooling effect described here. However, electron impact ionization can be driven with less deleterious effect by combining Rydberg excitation with the conventional method for plasma creation [7] in a double-pulse scheme. Here, the first laser pulse is tuned below threshold to excite strongly correlated Rydberg atoms while leaving the majority of atoms in the ground state. The second pulse, tuned above threshold, ionizes a fraction of the ground state atoms to produce a low-density plasma with energetic electrons that subsequently convert the Rydberg gas into a correlated plasma. Such double-pulse sequences have already been implemented for pump-probe experiments in Rydberg gases [45,81], to excite Rydberg atoms in a UNP [82,83], and to convert a Rydberg gas to a plasma [52]. The final degree of plasma correlations will depend on the parameters of the seed plasma, which raises interesting questions for future studies.

Several extensions of the proposed scheme appear worth pursuing. First, a correlated plasma with $T \lesssim 100$ mK seems well suited for subsequent laser cooling on the $Sr^+(5S_{1/2}) \leftrightarrow Sr^+(5P_{1/2})$ transition, which thus far was hampered by DIH out of the Doppler range. Second, long-range dipolar Rydberg interactions, induced by resonant pair-state couplings [84–86] or external electric fields [87], may give rise to atomic correlations that are closer to those of long-range interacting Coulomb systems and, therefore, may further enhance the coupling strengths of the resulting plasma. Here, higher order interactions give rise to an interesting, correlated excitation dynamics [86,88,89] that could be probed by monitoring Γ of the corresponding UNP. Finally, Rydberg excitation by standing-wave light fields is expected to increase atomic correlations substantially. If the lattice constant matches the blockade radius, we expect strong excitation ordering that could push Γ to values not far below the crystalline-plasma regime ($\Gamma \approx 174$ [1]).

[1] S. Ichimaru, Rev. Mod. Phys. **54**, 1017 (1982).
[2] R. Redmer, Phys. Rep. **282**, 35 (1997).
[3] D. H. E. Dubin and T. M. ONeil, Rev. Mod. Phys. **71**, 87 (1999).

[4] W. Baumjohann and R. A. Treumann, *Basic Space Plasma Physics* (World Scientific, Singapore, 1996).

[5] H. M. van Horn, Science **252**, 384 (1991).

[6] S. Atzeni and J. Meyer-Ter-Vehn, *The Physics of Inertial Fusion* (Larendon, Oxford, 2004).

[7] T. C. Killian, S. Kulin, S. Bergeson, L. Orozco, C. Orzel, and S. Rolston, Phys. Rev. Lett. **83**, 4776 (1999).

[8] T. C. Killian, T. Pattard, T. Pohl, and J. M. Rost, Phys. Rep. **449**, 77 (2007).

[9] T. C. Killian, Science **316**, 705 (2007).

[10] R. S. Fletcher, X. L. Zhang, and S. L. Rolston, Phys. Rev. Lett. **96**, 105003 (2006).

[11] J. Castro, P. McQuillen, and T. C. Killian, Phys. Rev. Lett. **105**, 065004 (2010).

[12] S. D. Bergeson and F. Robicheaux, Phys. Rev. Lett. **101**, 073202 (2008).

[13] G. Bannasch, J. Castro, P. McQuillen, T. Pohl, and T. C. Killian, Phys. Rev. Lett. **109**, 185008 (2012).

[14] X. L. Zhang, R. S. Fletcher, and S. L. Rolston, Phys. Rev. Lett. **101**, 195002 (2008).

[15] S. B. van der Geer, M. P. Reijnders, M. J. de Loos, E. J. D. Vredenbregt, P. H. A. Mutsaers, and O. J. Luiten, J. Appl. Phys. **102**, 094312 (2007).

[16] J. L. Hanssen, S. B. Hill, J. Orloff, and J. J. McClelland, Nano Lett. **8**, 2844 (2008).

[17] M. P. Reijnders, P. van Kruisbergen, G. Taban, S. van der Geer, P. Mutsaers, E. Vredenbregt, and O. Luiten, Phys. Rev. Lett. **102**, 034802 (2009).

[18] M. P. Reijnders, N. Debernardi, S. B. van der Geer, P. H. A. Mutsaers, E. J. D. Vredenbregt, and O. J. Luiten, Phys. Rev. Lett. **105**, 034802 (2010).

[19] B. Knuffman, A. V Steele, J. Orloff, and J. J McClelland, New J. Phys. **13**, 103035 (2011).

[20] N. Debernardi, R. W. L van Vliembergen, W. J. Engelen, K. H. M. Hermans, M. P. Reijnders, S. B. van der Geer, P. H. A. Mutsaers, O. J. Luiten, and E. J. D. Vredenbregt, New J. Phys. **14**, 083011 (2012).

[21] M. S. Murillo, Phys. Rev. Lett. **87**, 115003 (2001).

[22] D. O. Gericke, M. S. Murillo, D. Semkat, M Bonitz, and D. Kremp, J. Phys. A **36**, 6087 (2003).

[23] C. E. Simien, Y. Chen, P. Gupta, S. Laha, Y. Martinez, P. Mickelson, S. Nagel, and T. Killian, Phys. Rev. Lett. **92**, 143001 (2004).

[24] Y. C. Chen, C. Simien, S. Laha, P. Gupta, Y. Martinez, P. Mickelson, S. Nagel, and T. Killian, Phys. Rev. Lett. **93**, 265003 (2004).

[25] T. Pohl, T. Pattard, and J. M. Rost, Phys. Rev. Lett. **94**, 205003 (2005).

[26] E. A. Cummings, J. Daily, D. Durfee, and S. Bergeson, Phys. Rev. Lett. **95**, 235001 (2005).

[27] S. D. Bergeson, A. Denning, M. Lyon, and F. Robicheaux, Phys. Rev. A **83**, 023409 (2011).

[28] M. Lyon, S. D. Bergeson, and M. S. Murillo, Phys. Rev. E **87**, 033101 (2013).

[29] T. Pohl, T. Pattard, and J. M. Rost, J. Phys. B **37**, L183 (2004).

[30] D. O. Gericke and M. S. Murillo, Contrib. Plasma Phys. **43**, 298 (2003).

[31] P. K. Shukla and K. Avinash, Phys. Rev. Lett. **107**, 135002 (2011).

[32] M. D. Lukin, M. Fleischhauer, and R. Cote, Phys. Rev. Lett. **87**, 037901 (2001).

[33] T. F. Gallagher, *Rydberg Atoms* (Cambridge University Press, Cambridge, England, 1994).

[34] M. Robert-de-Saint-Vincent, C. S. Hofmann, H. Schempp, G. Günter, S. Whitlock, and M. Weidemüller, Phys. Rev. Lett. **110**, 045004 (2013).

[35] E. Urban, T. A. Johnson, T. Henage, L. Isenhower, D. D. Yavuz, T. G. Walker, and M. Saffman, Nat. Phys. **5**, 110 (2009).

[36] A. Gaëtan, Y. Miroshnychenko, T. Wilk, A. Chotia, M. Viteau, D. Comparat, P. Pillet, A. Browaeys, and P. Grangier, Nature Phys. **5**, 115 (2009).

[37] M. Saffman, T. G. Walker, and K. Molmer, Rev. Mod. Phys. **82**, 2313 (2010).

[38] J. D. Pritchard, D. Maxwell, A. Gauguet, K. J. Weatherill, M. P. A. Jones, and C. S. Adams, Phys. Rev. Lett. **105**, 193603 (2010).

[39] Y. O. Dudin and A. Kuzmich, Science **336**, 887 (2012).

[40] T. Peyronel, O. Firstenberg, Q.-Y. Liang, S. Hofferberth, A. V. Gorshkov, T. Pohl, M. D. Lukin, and V. Vuletić, Nature (London) **488**, 57 (2012).

[41] D. Maxwell, D. J. Szwer, D. Paredes-Barato, H. Busche, J. D. Pritchard, A. Gauguet, K. J. Weatherill, M. P. A. Jones, and C. S. Adams, Phys. Rev. Lett. **110**, 103001 (2013).

[42] V. Parigi, E. Bimbard, J. Stanojevic, A. J. Hilliard, F. Nogrette, R. Tualle-Brouri, A. Ourjoumtsev, and P. Grangier, Phys. Rev. Lett. **109**, 233602 (2012).

[43] C. S. Hofmann *et al.*, Phys. Rev. Lett. **110**, 203601 (2013).

[44] U. Raitzsch *et al.*, Phys. Rev. Lett. **100**, 013002 (2008).

[45] H. Schempp *et al.*, Phys. Rev. Lett. **104**, 173602 (2010).

[46] M. Viteau *et al.*, Phys. Rev. Lett. **107**, 060402 (2011).

[47] A. Schwarzkopf, R. E. Sapiro, and G. Raithel, Phys. Rev. Lett. **107**, 103001 (2011).

[48] P. Schauß *et al.*, Nature (London) **491**, 87 (2012).

[49] M. Viteau *et al.*, Phys. Rev. Lett. **109**, 053002 (2012).

[50] S. Laha *et al.*, Phys. Rev. Lett. **99**, 155001 (2007).

[51] J. Millen, G. Lochead, and M. P. A. Jones, Phys. Rev. Lett. **105**, 213004 (2010).

[52] P. McQuillen *et al.*, Phys. Rev. A **87**, 013407 (2013).

[53] G. Lochead *et al.*, Phys. Rev. A **87**, 053409 (2013).

[54] C. Ates, T. Pohl, T. Pattard, and J. M. Rost, Phys. Rev. A **76**, 013413 (2007); Phys. Rev. Lett. **98**, 023002 (2007); J. Phys. B **39**, L233 (2006).

[55] C. Ates, S. Sevinçli, and T. Pohl, Phys. Rev. A **83**, 041802 (2011).

[56] K. P. Heeg, M. Gärttner, and J. Evers, Phys. Rev. A **86**, 063421 (2012).

[57] M. Höning *et al.*, Phys. Rev. A **87**, 023401 (2013).

[58] C. Ates and I. Lesanovsky, Phys. Rev. A **86**, 013408 (2012).

[59] R. Mukherjee *et al.*, J. Phys. B **44**, 184010 (2011).

[60] C. L. Vaillant, M. P. A. Jones, and R. M. Potvliege, J. Phys. B **45**, 135004 (2012).

[61] H. Katori, T. Ido, Y. Isoya, and M. Kuwata-Gonokami, Phys. Rev. Lett. **82**, 1116 (1999).

[62] P. G. Mickelson *et al.*, Phys. Rev. Lett. **95**, 223002 (2005).

[63] Y. N. Martinez de Escobar *et al.*, Phys. Rev. Lett. **103**, 200402 (2009).

[64] For the parameters of this work ($\Omega_1 = 25$ MHz, $\Omega_2 = 0.5$ MHz, $t_{exc} = 0.5\ \mu$s) $\Delta\nu = 13.7$ MHz.

[65] J. G. Leopold and I. C. Percival, J. Phys. B **12**, 709 (1979).

[66] T. C. Killian *et al.*, Phys. Rev. Lett. **86**, 3759 (2001).

[67] R. S. Fletcher, X. L. Zhang, and S. L. Rolston, Phys. Rev. Lett. **99**, 145001 (2007).

[68] P. Gupta *et al.*, Phys. Rev. Lett. **99**, 075005 (2007).

[69] T. Pohl, D. Vrinceanu, and H. R. Sadeghpour, Phys. Rev. Lett. **100**, 223201 (2008).

[70] G. Bannasch and T. Pohl, Phys. Rev. A **84**, 052710 (2011).

[71] A. Wetzels *et al.*, Phys. Rev. Lett. **89**, 273003 (2002).

[72] H. Dachsel, J. Chem. Phys. **132**, 119901 (2010).

[73] For our typical electron temperatures and densities, electronic screening does not affect the ion temperature evolution [24] and can, therefore, be neglected.

[74] F. Robicheaux and J. V. Hernández, Phys. Rev. A **72**, 063403 (2005).

[75] M. P. Robinson *et al.*, Phys. Rev. Lett. **85**, 4466 (2000).

[76] F. Robicheaux and J. D. Hanson, Phys. Plasmas **10**, 2217 (2003).

[77] T. Pohl, T. Pattard, and J. M. Rost, Phys. Rev. A **68**, 010703 (2003).

[78] J. P. Morrison, C. J. Rennick, J. S. Keller, and E. R. Grant, Phys. Rev. Lett. **101**, 205005 (2008).

[79] T. M. Weber *et al.*, Phys. Rev. A **86**, 020702 (2012).

[80] T. Amthor *et al.*, Phys. Rev. Lett. **98**, 023004 (2007).

[81] A. Reinhard *et al.*, Phys. Rev. Lett. **100**, 233201 (2008).

[82] N. Vanhaecke *et al.*, Phys. Rev. A **71**, 013416 (2005).

[83] T. Pohl *et al.*, Eur. Phys. J. D **40**, 45 (2006).

[84] T. Vogt *et al.*, Phys. Rev. Lett. **97**, 083003 (2006).

[85] A. Reinhard *et al.*, Phys. Rev. Lett. **100**, 123007 (2008).

[86] K. C. Younge *et al.*, Phys. Rev. A **79**, 043420 (2009).

[87] T. Vogt, Phys. Rev. Lett. **99**, 073002 (2007).

[88] T. Pohl and P. R. Berman, Phys. Rev. Lett. **102**, 013004 (2009).

[89] D. Cano and J. Fortágh, Phys. Rev. A **86**, 043422 (2012).